

A Poisson Solver for Spreading Resistance Analysis

D. H. Dickey

(Received 20 February 1991; accepted 8 October 1991) This paper was presented at The First Int'l Workshop on the Measurement and Characterization of Ultra-Shallow Doping Profiles MCNC, Research Triangle Park, NC March 18-21, 1991

It has become evident in recent years that carrier concentration profiles measured on beveled surfaces with a spreading resistance probe might not accurately reflect the associated vertical dopant profiles. Carrier spilling, even in the absence of surface states, can move an on-bevel junction 1/2 micron or more from its metallurgical depth. This paper describes a Poisson solver which we have developed for use in spreading resistance data reduction. It allows the calculation of dopant profiles from measured on-bevel profiles. Examples from a variety of structures are given.

Introduction

The use of spreading resistance analysis (SRA) to obtain carrier concentration profiles along a beveled surface has been an accepted method for approximating vertical dopant profiles for many years. More recently, it has become clear that although the method is highly adequate for many structures, it introduces systematic and predictable errors on other, mainly shallow and lightly doped, structures. A number of authors¹⁻⁴ have pointed out that the explanation lies simply in space-charge effects in the profile region, which in turn are adequately described by the one-dimensional Poisson equation. Thus a solution to Poisson's equation using on-bevel carrier concentration as input data is all that is required to obtain true dopant profiles from SRA. We have devised a relatively efficient one-dimensional Poisson solver which is reversible; i.e., it can be used to obtain carrier concentrations from dopant concentrations, or for the reverse procedure.

Because of the non-linearities in Poisson's equation, its solution can have a great susceptibility to noise in the input data. This is especially true when going in the reverse (carrier to dopant) direction. We deal with this problem by using a simple simulation procedure rather than rely on data smoothing alone.

The Poisson Solver

The basis of our solution is a straightforward numerical procedure in which we write Poisson's equation as a recursion relation and make use of known boundary conditions to set up the recursion process. The working formula is:

$$V_{j+1} - 2V_j + V_{j-1} = h^2 C [N_{A_j} - N_{D_j} + n_j - p_j] \quad (1)$$

The index j increases from surface to substrate, and denotes an absolute depth below the original sample surface. The potentials V_j are expressed in units of kT , so that the proportionality constant C has the numerical value:

$$C = q / \epsilon kT = 6 \times 10^{-6} \quad (2)$$

The depth increment h is in cm, and the concentrations are all in cm units. The electron concentration n_j is given by:

$$n_j = n_i \exp(V_j - V_f) \quad (3)$$

where V_f is the Fermi potential. The hole concentration p_j is obtained from the usual relation $np = n_i^2$. To begin the recursion process, the local surface potential is taken as zero, and the potential gradient at the local surface is defined in terms of any assumed surface charge density according to:

$$dV = 6 \times 10^{-6} h Q_{ss} \quad (4)$$

In the case of a forward solution, a trial value for the Fermi potential is taken and successive values of V_{j+1} , V_{j+2} , etc. are found from Eq.(1). If the Fermi potential is not precisely correct, an unreasonably large value of V will be found at some point before substrate is reached. When this occurs, a new value for the Fermi level is tried, and the recursion process is restarted at the local surface. A binary search method is used to adjust the trial Fermi potential. The Fermi level is further adjusted until the substrate boundary condition is satisfied. This condition requires that both sides of Eq.(1) vanish. When all of this is done, one has a solution for the vertical carrier concentration profile under the local surface, and can then move to the next location on the bevel and begin again.

For a reverse solution, in which dopant concentrations are found from carrier concentrations, the Fermi potentials are known. In this case, although the recursion on Eq.(1) still proceeds from local surface toward substrate, the process must begin with the point on the bevel which is nearest the substrate. With the surface potential at this point still zero and the surface potential gradient defined in terms of assumed surface charge density, a trial value of $N_A - N_D$ is adjusted until the substrate boundary condition is satisfied. The final value of $N_A - N_D$ obtained for this depth is then used in the recursion process for the next shallower point.

The reverse solution, especially in structures consisting of a simple junction above a uniformly doped substrate, can be extremely sensitive to noise in the data for those points in that region just below the junction. The solution is also critically dependent on the accuracy of the spreading resistance correction scheme in this region. We avoid much of these difficulties by making a minimal simulation of the dopant profile tail in this region. The simulation consists of constructing a Gaussian dopant distribution which, when used in a forward solution, results in a calculated carrier concentration which agrees exactly with the measured value at one point (called the splice point) near the junction. All dopant concentration values

below the splice point are taken from the Gaussian simulation, while those above are calculated from Eq.(1) as described above. A Gaussian can be completely characterized by three parameters: a peak concentration, a peak location and a half-width. For the simulation, the peak concentration and location are estimated from the measured profile, and the splice point is chosen as a "reliable" point just above the junction. Criteria for

choosing the splice point are discussed in the following section. A trial value of half-width is adjusted until a forward solution for the region between the splice point and substrate results in agreement with the measured concentration at the splice point. The dopant tail thus defined is used in the recursion process for continuing the reverse solution on up to the original sample surface.

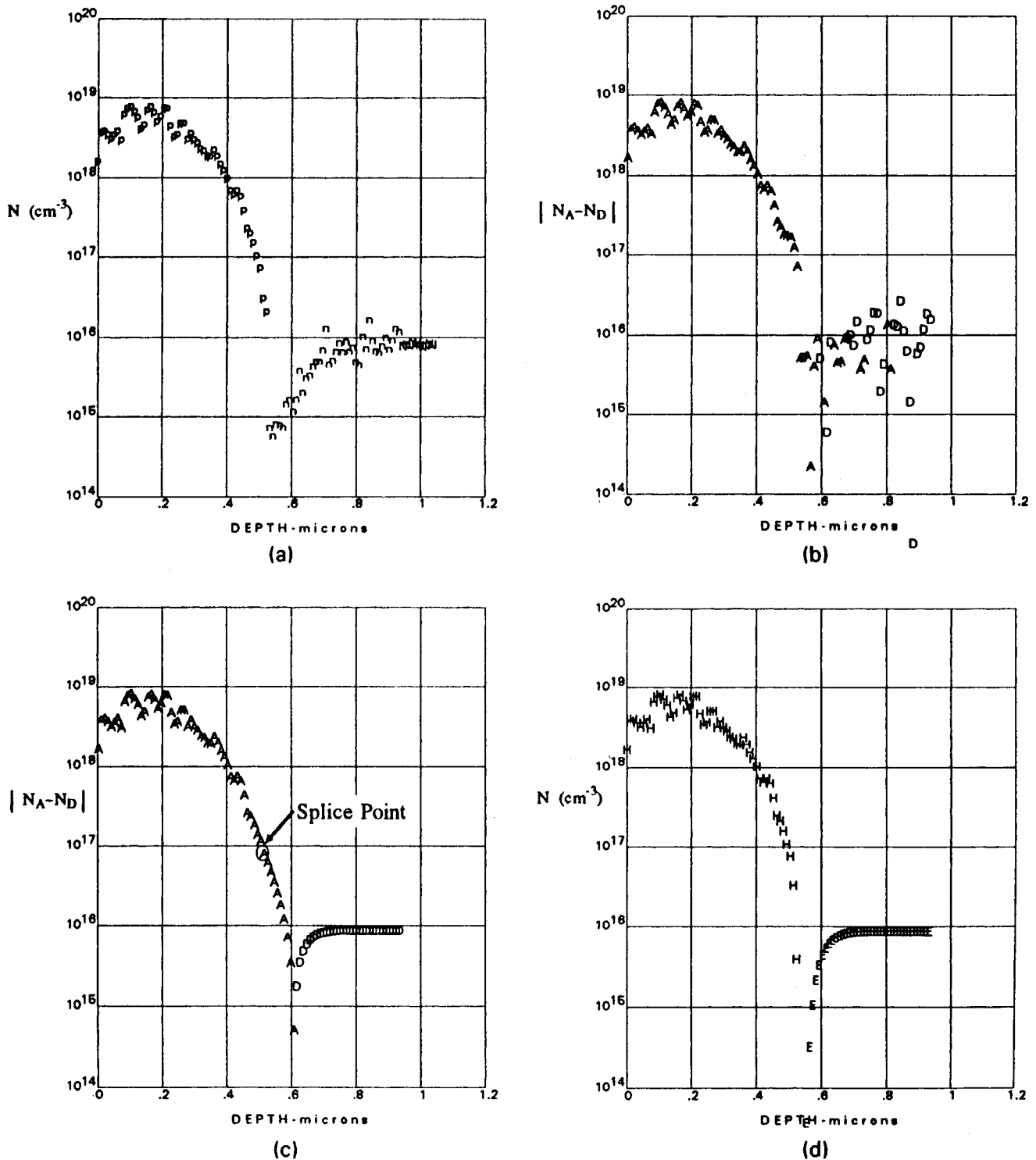


Figure 1. A boron base implant
 (a) Measured on-bevel carrier concentration,
 (b) Dopant profile obtained from unsmoothed carrier concentration. A denotes that $N_A - N_D$ is positive, D denotes that $N_A - N_D$ is negative.
 (c) Dopant profile obtained using simulation.
 (d) Carrier concentration re-calculated from profile in (c). H denotes holes as majority carrier. E denotes electrons.

Applications

The measured on-bevel carrier concentration profile for a boron base implant is shown in Figure 1(a). Using a direct solution of Poisson's equation with the data of Figure 1(a) as input results in the dopant profile of Figure 1(b). The noise sensitivity of the process is evident. With a dopant tail simulated from a depth of $0.50\ \mu\text{m}$ down to the maximum depth reached, a reverse solution results in the profile shown in Figure 1(c). Note that, although the simulating Gaussian used has peak concentration and location based on values near the surface in Figure 1(a), only the tail (from $0.50\ \mu\text{m}$ down) is actually used. As a check on the accuracy of the procedure, the data of Figure 1(c) was used as input for a

forward solution. This result, which should agree closely with the original data, is shown in Figure 1(d). We note that there is good agreement except right at the junction. The discrepancy near the junction is wholly expected, inasmuch as we have always suspected that measured spreading resistance values right at an on-bevel junction could be greatly in error. In other words, we believe that Figure 1(d), as a representation of an on-bevel profile, is more correct than Figure 1(a)! This discrepancy near the junction provides us some guidance in choosing the deepest possible point to take as a splice point: those points at and just below the on-bevel junction cannot be taken as reliable, but reliability improves rapidly as one moves back up toward the surface. The default choice made by our program is the second point above the junction.

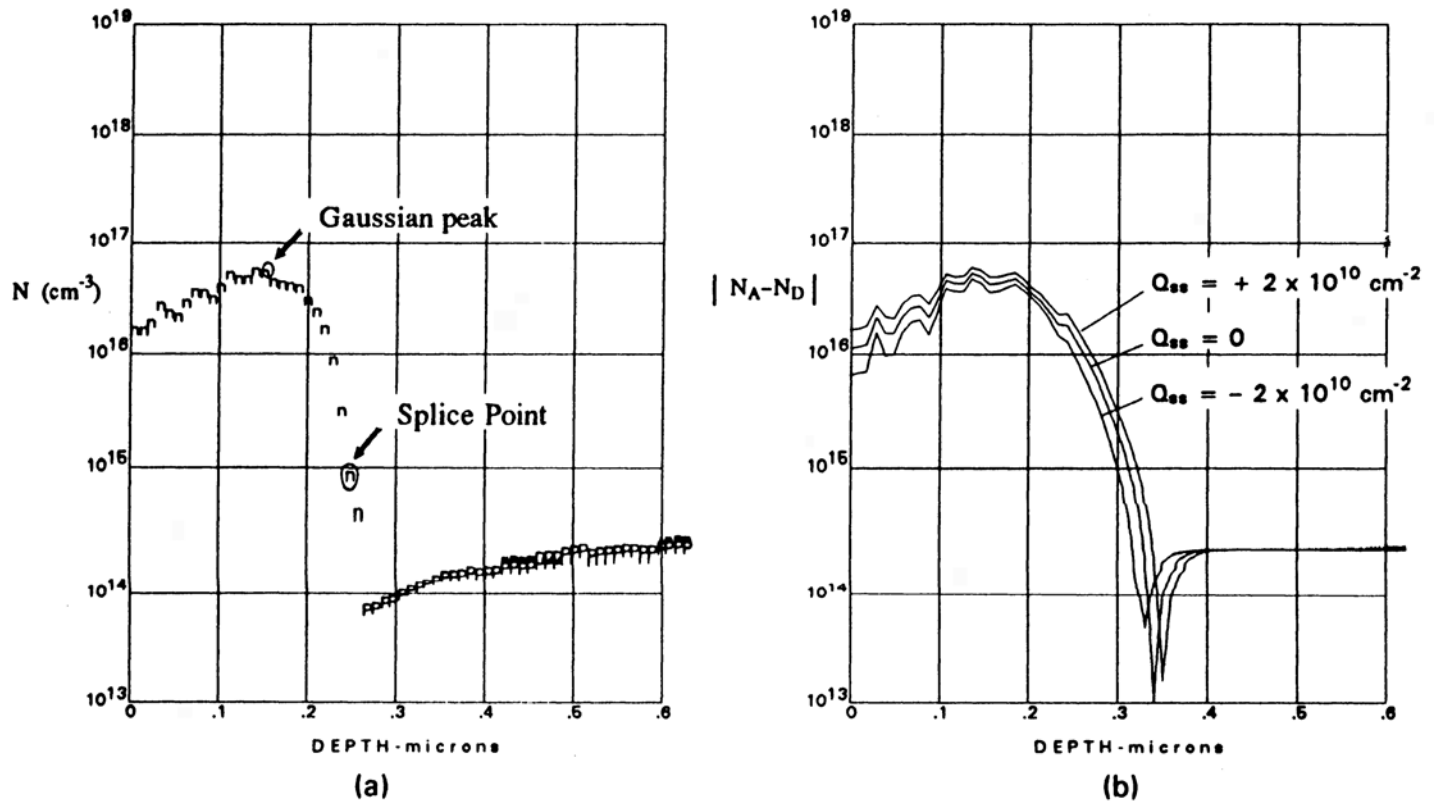


Figure 2. A high energy phosphorus implant.

(a) Measured on-bevel carrier concentration.

(b) Dopant profile obtained using simulation, for three different values of surface state density.

Another application is one in which surface state densities are introduced. The profile is that of a high-energy phosphorus implant, and the measured on-bevel profile is shown in Figure 2(a). Using a Gaussian simulation of the phosphorus tail from $0.25\ \mu\text{m}$ down, with the indicated peak location, the dopant profiles in Figure 2(b) were obtained. The three curves

correspond to assumed surface state densities of 2×10^{10} , 0 , and $-2 \times 10^{10}\ \text{cm}^{-2}$. We note that the introduction of non-zero surface state density shifts the entire profile, and allows the possibility of matching the result with an independent measure of either integrated charge or of sheet resistance.

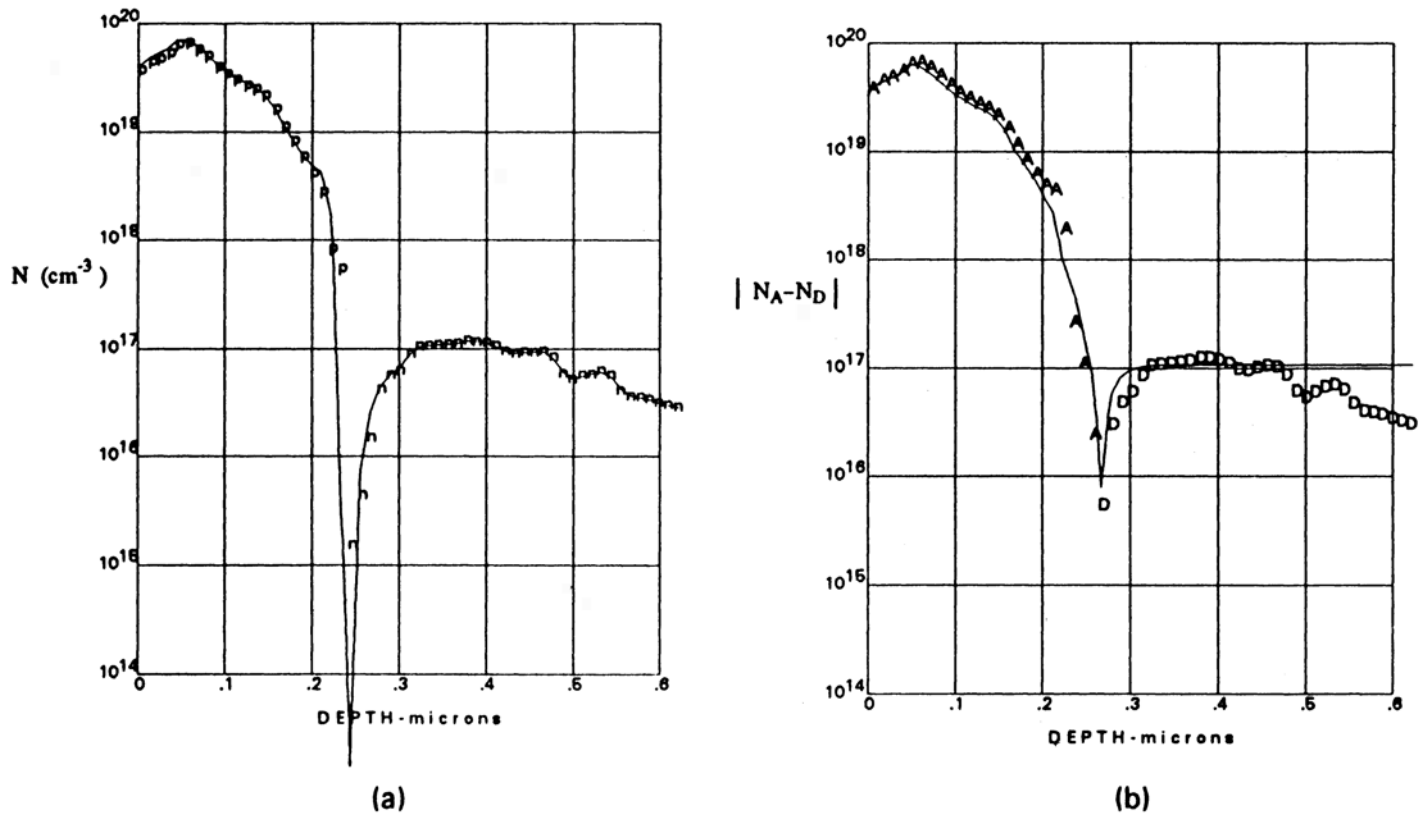


Figure 3. A boron source implant into n-well.

- (a) Symbols = the measured on-bevel profile. Solid lines = the on-bevel profile calculated from direct solution.
 (b) Symbols = dopant profile obtained by direct solution. Solid lines = dopant profile obtained using simulation.

The final example is a boron source implant into an n-well. The on-bevel carrier concentration is plotted with symbols in Figure 3(a). Because the region below the junction is not uniformly doped and because we have carefully smoothed the data in this region, we have succeeded in getting a reverse solution without resorting to simulation. This result is shown in Figure 3(b). Using this direct solution as input, we have recalculated the on-bevel profile shown as the solid curve in Figure 3(a). As in the first example, there is good agreement with measured values except right at the on-bevel junction. Finally, in Figure 3(b), we show the dopant profile obtained from the simulation, as a solid curve. The agreement between the two differently derived curves in Figure 3(b) is taken as evidence that either result is valid.

Conclusions

The use of a simple simulation process has been shown to be a viable way of obtaining reverse solutions of Poisson's equation. The alternate choice of using careful data smoothing has also been demonstrated, but it unfortunately cannot be

relied upon in all applications. The more one knows about the physical process used to create the profile, the safer it is to rely on simulation. The procedures described here were developed to satisfy a need for on-line calculation of dopant profiles from on-bevel carrier concentration data acquired with a spreading resistance probe. Although there is a potential application for a Poisson solver in the actual spreading resistance data reduction process, no attempt has yet been made to apply our procedures there. A more urgent problem is to extend this work to two dimensions, so that different surface state densities on sample surface versus bevel surface can be adequately accounted for.

References

- 1) A. Casel and H. Jorke, *Appl. Phys. Lett.* 50, 989 (1987)
- 2) S. M. Hu, *J. Appl. Phys.* 53, 1499 (1982)
- 3) W. Vandervorst and T. Clarysse, *J. Electrochem. Soc.* 137, 679 (1990)
- 4) J. Albers, "Emerging Semiconductor Technology", Gupta and Langer, eds, ASTM STP 960, 480 (1986)